Cytometrical Evidence That the Loss of Seed Weight in the *miniature1* Seed Mutant of Maize Is Associated with Reduced Mitotic Activity in the Developing Endosperm[1]

Barbara Vilhar, Aleš Kladnik, Andrej Blejec, Prem S. Chourey, and Marina Dermastia*

Department of Biology, Biotechnical Faculty, University of Ljubljana, Vecna pot 111, SI–1001 Ljubljana, Slovenia (B.V., A.K., M.D.); National Institute of Biology, Vecna pot 111, SI–1001 Ljubljana, Slovenia (A.B.); and University of Florida and United States Department of Agriculture, Agricultural Research Service, Gainesville, Florida, 32611–0680 (P.S.C.)

"If you know a thing only qualitatively, you know it no more than vaguely. If you know it quantitatively—grasping some numerical measure that distinguishes it from an infinite number of other possibilities—you are beginning to know it deeply." (C. Sagan, Billions and Billions, 1997).

Using new approaches to quantitative image analysis, we provide the first direct evidence, to our knowledge, that loss of seed weight in the maize (*Zea mays*) *miniature1* (*mn1*) seed mutant is associated with reduced mitotic activity and inhibited cell expansion, whereas there are no alterations in the progress of endoreduplication in the mutant compared with the wild-type endosperm. Furthermore, we contribute substantial new information about the spatial distribution of various developmental processes at the cellular level in the maize endosperm.

Enlargement of the maize endosperm relies upon two cellular processes: cell division and cell expansion, which is in turn related to endoreduplication of nDNA (Kondorosi et al., 2000; Larkins et al., 2001). Intense mitotic activity occurs between 8 and 14 DAP (days after pollination; Kowles and Phillips, 1985; Schweizer et al., 1995). Cell division ceases in the central endosperm by about 12 DAP, but continues until late developmental stages in the peripheral cell layers, away from the embryo (Kiesselbach, 1949; Kowles and Phillips, 1985, 1988). Endoreduplication begins at 10 DAP (Kowles and Phillips, 1985; Schweizer et al., 1995). The highest nDNA amount, expressed as C value, is typically 96C to 192C, as quantified by measurements of the nuclear volume (Tschermak-Woess and Enzenberg-Kunz, 1965), Feulgen cytophotometry (Kowles and Phillips, 1985), and flow cytometry (Kowles et al., 1992; Schweizer et al., 1995; Larkins et al., 2001; Settler and Flannigan, 2001). In the period between 12 and 15 DAP, storage products start to accumulate (Tsai et al., 1970). The total number of endosperm cells at 16 DAP has been measured with flow cytometry (Kowles et al., 1992; Schweizer et al., 1995; Settler and Flannigan, 2001) or with nuclei counts after digestion of the endosperm with cell wall degrading enzymes (Jones et al., 1985) and is estimated to be 54,000 to 700,000.

The *mn1* seed mutant shows a drastic reduction in endosperm size compared with that of the wild type, *Mn1*, with the weight of the mature *miniature* endosperm being only 20% that of the wild type (Lowe and Nelson, 1946). The causal basis of the *mn1* seed phenotype is the loss of cell wall invertase, INCW2, encoded by the *Mn1* gene (Miller and Chourey, 1992; Cheng et al., 1996), which is specifically expressed at the base of the endosperm (Cheng et al., 1996). In both maize and fava bean (*Vicia faba*), cell wall invertase cleavage of Suc during the early stages of seed development is believed to play a critical role in providing hexose sugars to maintain mitotic division and only a minor role in providing substrates for starch biosynthesis (Weber et al., 1997; Cheng and Chourey, 1999). Indirect evidence suggests that in the maize endosperm, the peak of INCW2 activity at 12 DAP temporally coincides with the phase of intense cell divisions in the endosperm (Cheng et al., 1996; Cheng and Chourey, 1999). However, it has never been directly demonstrated that INCW2 deficiency in the *mn1* maize endosperm is associated with reduced mitotic activity.

To investigate whether the small size of the *mn1* endosperm is a consequence of impaired mitosis, cell expansion, or endoreduplication, we compared cytological parameters in homozygous *Mn1* (wild-type) and *mn1* (*miniature*) kernels of the W22 inbred line of maize harvested at 16 DAP. We analyzed the spatial distribution of cells by sizes and endopolyploidy levels (C values) in longitudinal sections of the endosperm using image cytometry. On the basis of the longitudinal sections, we constructed a three-dimensional (3-D) model of the endosperm.

[1] This work was supported by the USA-Slovenia cooperation in science and technology grant no. 331–01–838050 and Mercator d.d. (travel grant). A.K. is a recipient of a PhD grant from the Ministry of Education, Science, and Sport (Republic of Slovenia; grant no. S1–487–001/20070/99). This paper is Florida Agricultural Experimental Journal Series no. R–08656.

* Corresponding author; e-mail marina.dermastia@uni-lj.si; fax 386–12573390.

www.plantphysiol.org/cgi/doi/10.1104/pp.001826.

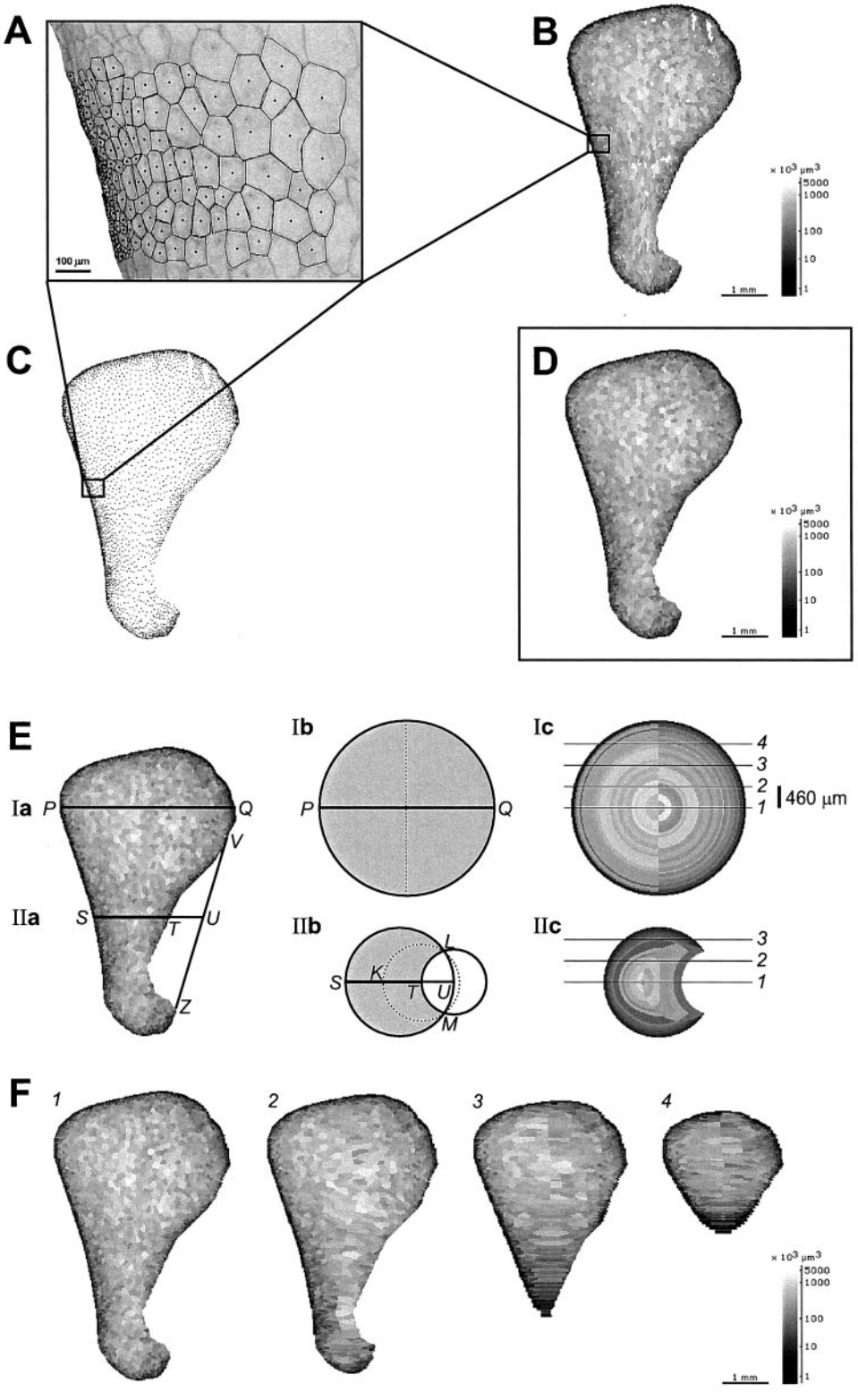

Figure 1. Construction of the 3-D model of the endosperm. A through D, Estimation of cell volume and nDNA amount on the 2-D longitudinal section. E and F, Extrapolation from 2-D data to the 3-D endosperm model. For explanation of figures, see "The 3-D Model of the Endosperm."

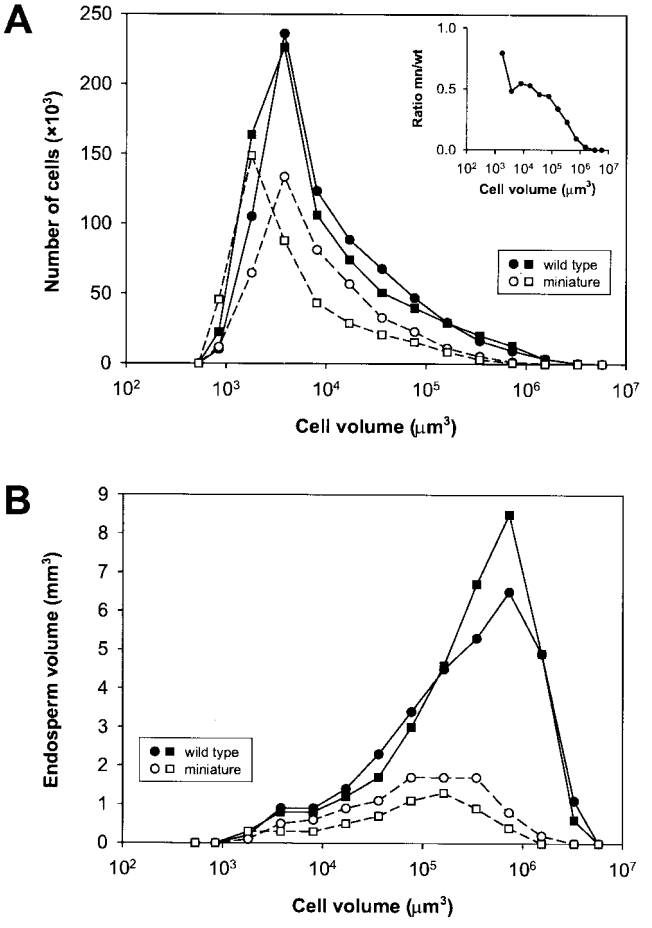

Figure 2. Structure of the wild type and the *miniature* endosperm in relation to the cell volume. Two 16-DAP kernels of each genotype were compared using the 3-D model of the endosperm. A, Distribution of cell volumes in the endosperm. Inset shows the ratio between the mean number of cells in the *miniature* and in the wild-type endosperm at respective cell volume classes. B, Volume of endosperm occupied by cells with different cell volumes. A and B, Wild-type kernel no. 1 (●; total number of cells 738,000; total endosperm volume 31.4 mm^3); wild-type kernel no. 2 (■; 751,000 cells; 33.2 mm^3); *miniature* kernel no. 1 (○; 422,000 cells; 9.3 mm^3); and *miniature* kernel no. 2 (□; 404,000 cells; 6.0 mm^3). Cell volume is shown in logarithmic scale.

THE 3-D MODEL OF THE ENDOSPERM

The endosperm model was based on measurement of the cell area and nDNA amount on the endosperm median longitudinal section. The same Feulgen-stained section was used for cell area and nDNA amount measurements. Image analysis instrumentation was as by Vilhar et al. (2001). For all described measurements, we developed macros based on the KS400 image analysis software package (Carl Zeiss Vision, Munich).

To estimate the cell volume and nDNA amount on the two-dimensional (2-D) longitudinal section (Fig. 1, A–D), we interactively outlined the cell walls of individual cells on the image grabbed from a microscope (Fig. 1A). For each cell, we recorded its position (centroid coordinates shown as dots in Fig. 1A) and measured the cell area. The cell volume was estimated from the cell area, assuming that each cell was a sphere. The cell volume data were shown as gray values on the image (Fig. 1B). To overcome the problem of missing data (areas where no cells have been outlined; white regions in Fig. 1B), the image of the longitudinal section was reconstructed with the virtual cellularization method (Fig. 1D), an adapted version of the random sets mosaic method (Matérn, 1960). Each pixel in the endosperm was assigned to its nearest cell outline centroid (Fig. 1C), which led to separation of the endosperm into virtual cells. To each virtual cell, the cell volume of its respective centroid was assigned. The cell volumes were displayed as gray values (Fig. 1D; note the almost identical pattern of gray values in B and D and the absence of areas with missing data in D compared with B). A similar procedure, based on C-value data instead of cell area, was used to construct the image showing nDNA amounts. Hence, using virtual cellularization, both the cell volume and the C value were assigned to each virtual cell on the analyzed section.

The next step of model construction was extrapolation from 2-D data to the 3-D endosperm model (Fig. 1, E and F). The image shown in Figure 1D was the 2-D basis for estimation of distribution of cells in 3-D. The longitudinal section was, in essence, rotated around its longitudinal axis. To correct for the irregular 3-D shape of the endosperm, the endosperm was not rotated as a whole. Instead, the image of the longitudinal section was sliced along the *y* axis, with slice thickness of 1 pixel. For each pixel line (Fig. 1E, Ia line *PQ* and IIa line *ST*), a virtual cross-section composed of voxels was created (Fig. 1E, Ib and IIb). The area of the virtual cross-section was filled in with gray values (Fig. 1E, Ic and IIc) on the basis of the gray-value profile along the selected pixel line. For pixel lines in the regions without the embryo pocket, the assumed cross section was a circle with the diameter equal to distance *PQ* (Fig. 1E, Ia and Ib). The gray-value profile was rotated for ±90°, resulting in concentric bands of voxels with the same gray value (Fig. 1E, Ic). For pixel lines in the region with the embryo pocket, the extreme points at the top and bottom of the embryo pocket were first connected with a straight line (Fig. 1E, line *VZ*). The distance *TU* was assumed to be the radius of the embryo pocket circle, whereas the distance *SU* corresponded to the diameter of the endosperm circle (Fig. 1E, IIa and IIb). The sizes of cells surrounding the embryo pocket were different from the outer layers of the endosperm bordering with the pericarp (Fig. 5A). Hence, the "region of embryo influence" was defined as a circle based on three points (Fig. 1E, IIb, dashed line): the midpoint of the gray-value profile (*K*) and the intercepts between the endosperm circle

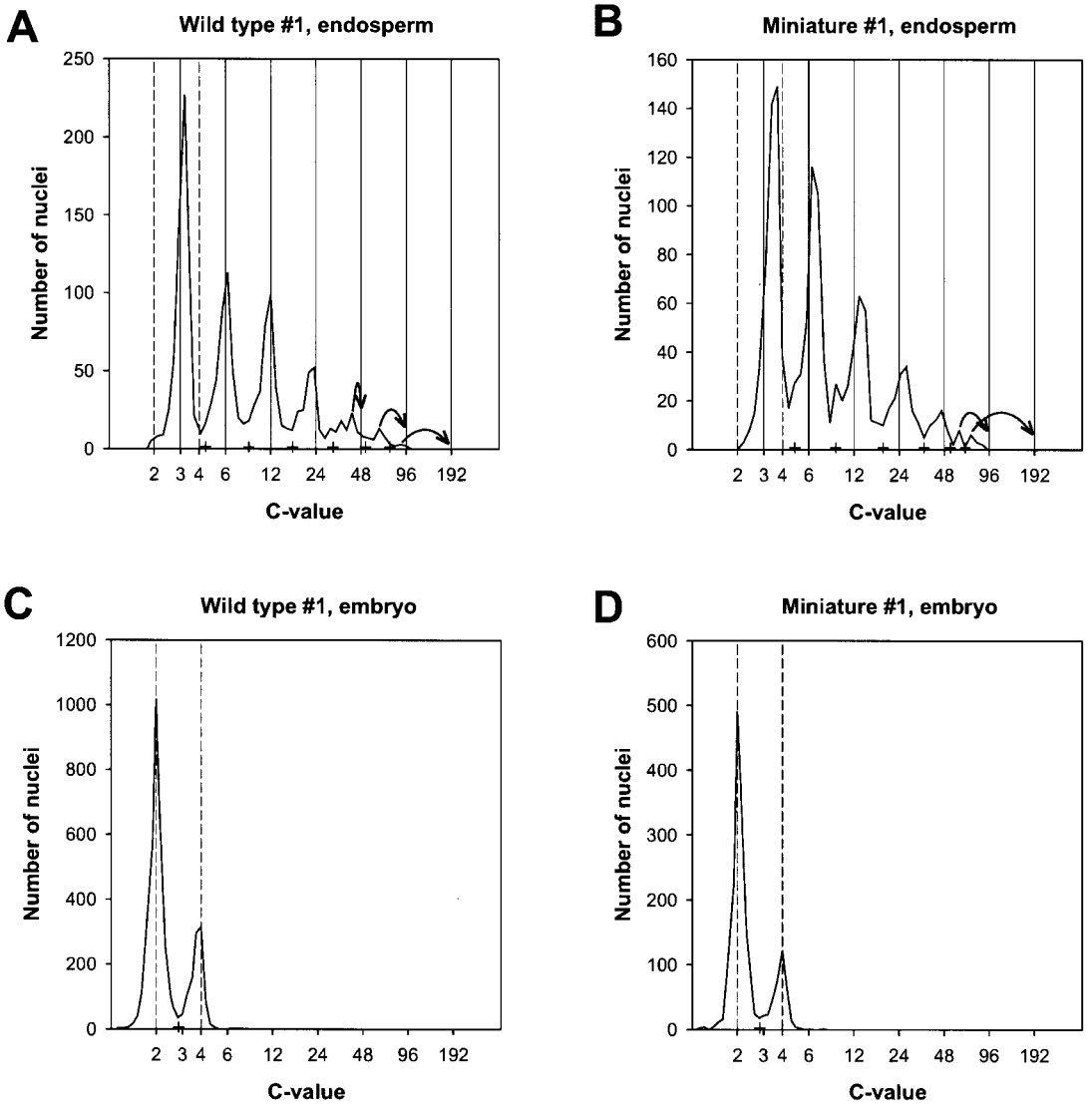

Figure 3. Frequency distribution of nDNA amounts in longitudinal sections of the wild type (A and C) and the *miniature* mutant (B and D) in endosperm (A and B) and in embryo (C and D) of 16-DAP kernels. DNA was quantitatively stained with the Feulgen reaction (Greilhuber and Ebert, 1994), and permanent slides were prepared (Vilhar et al., 2001; the KS400 protocol). For each nucleus, tissue type (embryo or endosperm), position (centroid coordinates of the nucleus), nuclear area, and nDNA amount were recorded. nDNA amount was measured with DNA image cytometry following the interphase-peak method (Vilhar et al., 2001; Vilhar and Dermastia, 2002). The distribution of nDNA amounts for the embryo cells (C and D) showed two peaks, corresponding to the 2C and 4C value (dashed lines). The mode of the embryo 2C peak was used as an internal calibration standard for conversion of the nDNA amount data from arbitrary units to C values. The limits between two consecutive peaks were set at midpoint between their modes (crosses on the *x* axis), allowing each nucleus to be assigned to a certain DNA replication level (C-value class). Arrows on A and B indicate misplacing of the high C-value peaks. At high C values, a part of the nucleus was not contained on the section, because the nuclear diameter was larger than section thickness (20 μm). A, 1,658 nuclei; B, 1,331 nuclei; C, 4,231 nuclei were measured; and D, 1,862 nuclei.

and the embryo pocket circle (*L* and *M*). The gray-value bands were fitted into the virtual cross section (example in Fig. 1E, IIc). The gray values from *KT* were used for voxels within the region of embryo influence, and those from *SK* were used for all other endosperm voxels. Examples of virtual serial longitudinal sections generated with the described 3-D model are presented in Figure 1F (*1*, *2*, *3*, and *4* correspond to respective labels in Fig. 1E). The described 3-D model of the endosperm enabled construction of frequency distribution of the voxel gray values, which was used to estimate the total number of cells in the endosperm. The number of cells at different endopolyploidy levels was calculated according to the above procedure, using the images shown in Figure 5B as the basis for 3-D modeling.

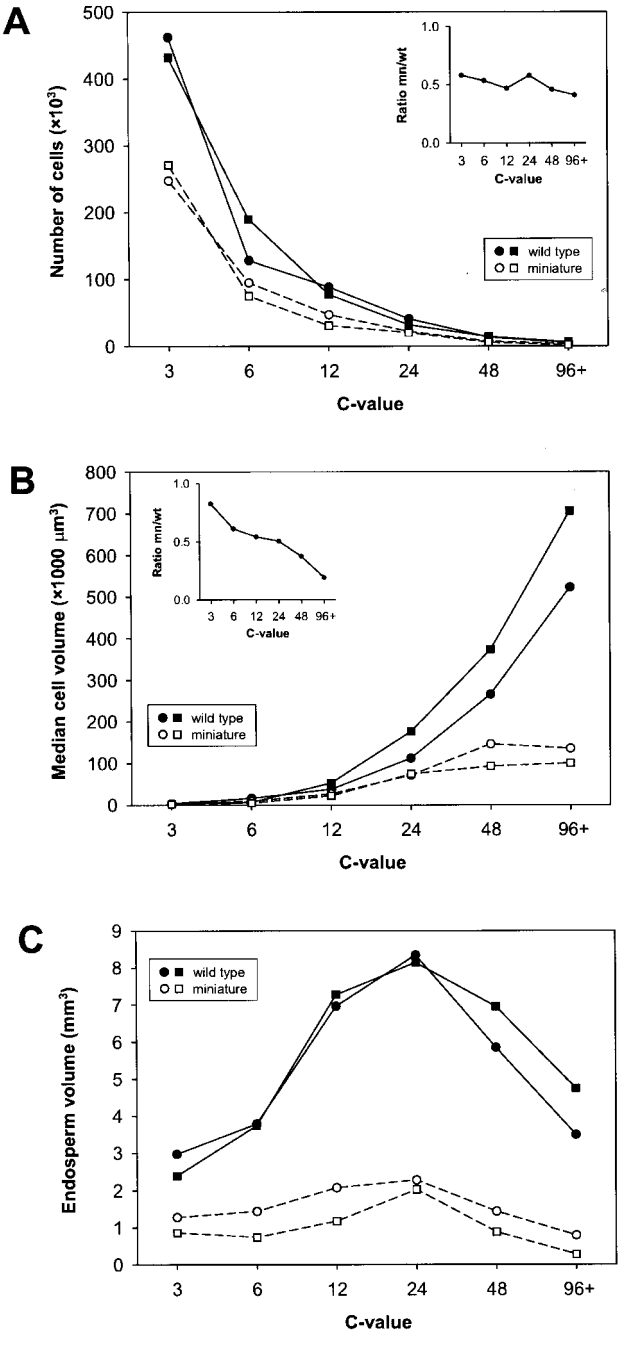

Figure 4. Structure of the wild type and the *miniature* endosperm in relation to DNA replication levels. Two 16-DAP kernels of each genotype were compared using the 3-D model of the endosperm. A, Distribution of cells belonging to different C-value classes; inset shows the ratio between the number of cells in the *miniature* and in the wild-type endosperm at respective C-value classes. B, The median cell volume of cells belonging to different C-value classes; inset shows the ratio between the median cell volume in the *miniature* and in the wild-type endosperm at respective C-value classes. The ratio shown in insets was calculated on the basis of the mean value of the respective parameters for each genotype. C, Volume of endosperm occupied by cells belonging to different C-value classes. A through C, Wild-type kernel nos. 1 and 2 (● and ■); *miniature* kernel nos. 1 and 2 (○ and □). The data for the 96C and the 192C class were pooled together due to a small number of cells. C value is shown in logarithmic scale.

CYTOLOGICAL PARAMETERS IN THE WILD TYPE AND *MINIATURE* ENDOSPERM

The total endosperm volume, estimated with the 3-D model, was 31 mm^3 consisting of 740,000 cells in the wild-type kernel and 8 mm^3 with 410,000 cells in the *miniature* kernel. Compared with the wild type, the number of cells in the *miniature* endosperm was 55%, whereas the endosperm volume was only 25%, indicating that in addition to impaired cell proliferation, there is also a reduction in the cell size contributing to the smallness of the *mn1* endosperm (Fig. 2).

The distribution of cell volumes was asymmetrical in both genotypes, with the majority of cells having a relatively small cell volume (Fig. 2A). However, compared with wild type, the *miniature* endosperm was deficient in the number of large cells (Fig. 2A, inset). Although most of the endosperm was occupied by large cells in both genotypes, increasing deficiency in the number of cells at increasing cell size resulted in the severely decreased total volume of the *miniature* endosperm (Fig. 2B).

At least six endoreduplication cycles were completed by 16 DAP in the endosperm of both genotypes (Fig. 3), showing that the progress of endoreduplication was not affected in the *miniature* endosperm compared with the wild type. The distribution of cells at a certain endopolyploidy level (C-value class) showed the same pattern in both genotypes (Fig. 4A), except that the number of cells in each C-value class in the *miniature* endosperm was only 40% to 60% that of the wild type (Fig. 4A, inset), in agreement with the overall deficiency in the total number of cells in the *miniature* endosperm (Fig. 2). In a previous study, 35 defective kernel mutants in maize (Kowles et al., 1992) were found to have both reduced cell numbers and reduced endopolyploidy levels, with the exception of one mutant that had a reduced cell number but functional endoreduplication. The *miniature* mutant is another example of the latter type of defective kernel mutation. Reduced number of cells together with functional endoreduplication in the *miniature* endosperm demonstrates that mitosis and endoreduplication are not directly coupled processes in the maize endosperm, as previously noted by Kowles et al. (1992).

A positive correlation between the cell volume and the amount of nDNA in both genotypes showed that cell enlargement and endoreduplication are interdependent processes (Fig. 4B). However, the median cell volume at each endopolyploidy level was smaller in the *miniature* than in the wild-type endosperm. The ratio between the cell volume in the *miniature* and the wild-type endosperm decreased with increasing endopolyploidy level (Fig. 4B, inset), indicating that in the *miniature* mutant cell expansion was particularly impaired at high endopolyploidy levels. Cells at 12C to 48C values occupied the largest part of the endosperm volume in both genotypes. Nevertheless, the absolute endosperm volume belonging to each

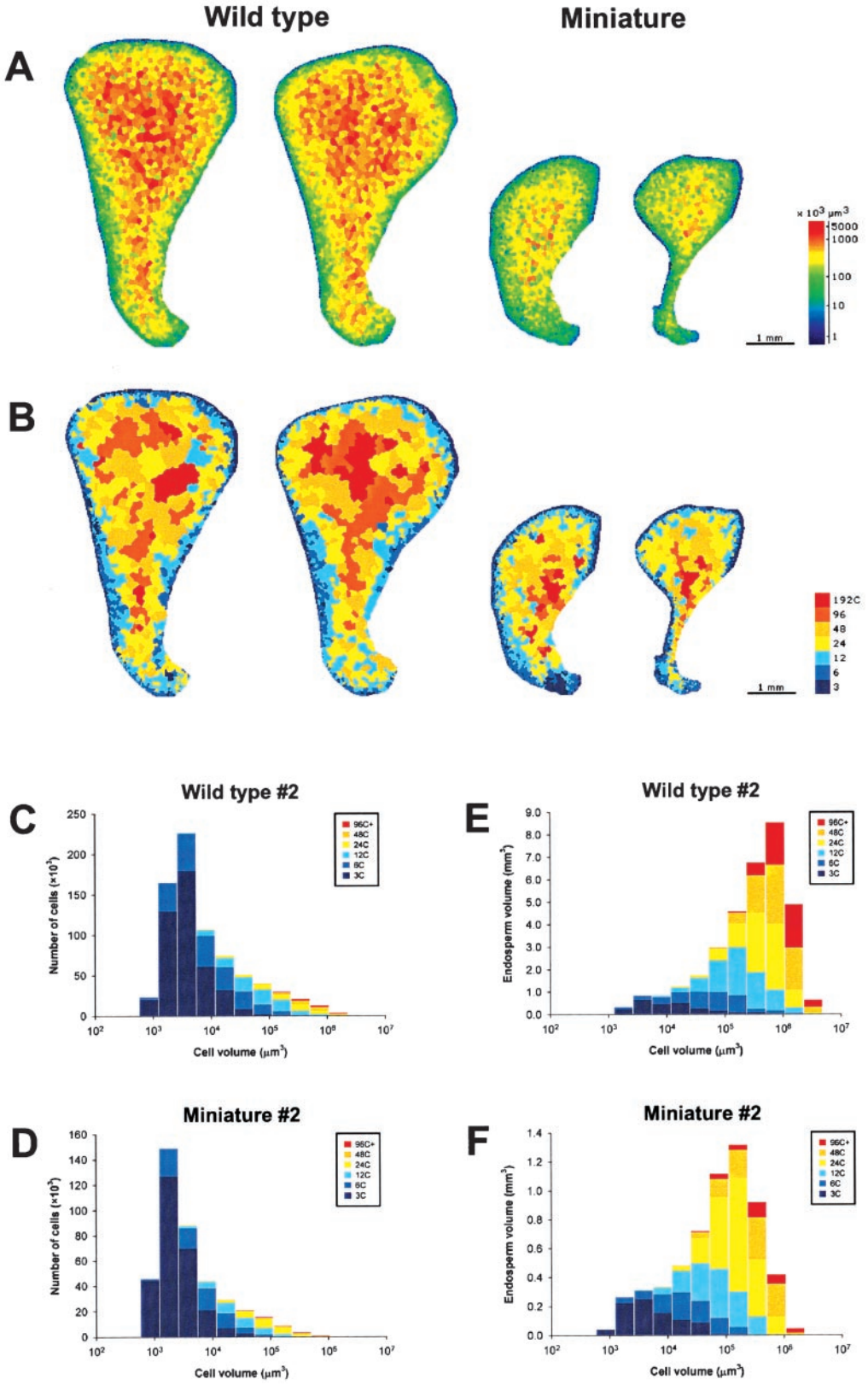

Figure 5. Structure of the wild-type and the *miniature* endosperm. Two 16-DAP kernels of each genotype were compared. A, Spatial distribution of cells with different volumes on the longitudinal section of the endosperm; images generated with the virtual cellularization method; for better visual perception, cell volumes calculated as gray values (see Fig. 1D) are shown

(*Legend continues on facing page.*)

Figure 5. (*Legend continued from facing page.*)
in pseudocolor scale. Sections from left to right, Wild-type kernel no. 1 (3,788 cells were outlined on the longitudinal section), wild-type kernel no. 2 (3,592 cells), *miniature* kernel no. 1 (2,974 cells), and *miniature* kernel no. 2 (2,660 cells). B, Spatial distribution of cells at different DNA replication levels on the longitudinal section of the endosperm; images generated with the virtual cellularization method; C values are shown in pseudocolor scale; sequence of sections is the same as in A. C and D, Stacked histograms showing the number of cells in relation to the cell volume and the DNA replication level. E and F, Stacked histograms showing the endosperm volume occupied by cells with different cell volumes and the DNA replication levels. C through F, Data obtained with the 3-D model of the endosperm; the data for the 96C and the 192C class were pooled together due to a small number of cells.

endopolyploidy level was smaller in the *miniature* than in the wild-type kernel (Fig. 4C), due to a combined effect of a reduced number of cells and a reduced cell size.

The histograms in Figure 5, C through F, show the complex relationship among the number of cells, the cell size, and the endopolyploidy level in the maize endosperm. The structural patterns were similar in both investigated genotypes with two exceptions: The *miniature* endosperm was characterized by smaller cells at respective endopolyploidy levels than the wild type, and by the absence of the largest cells. Although large cells at higher endopolyploidy levels were not numerous in either genotype, they contributed most to the final volume of the endosperm and were, thus, essential for endosperm enlargement. For example, only 7% of cells in the wild-type kernel had the nDNA amount of 24C value or higher, but these cells comprised 60% of the total endosperm volume (Fig. 5, C and E). The cells with 3C and 6C nDNA amounts had a share of 80% in the total number of cells; yet, they only contributed 20% to the total endosperm volume.

In both genotypes, the smallest cells were located in the outer layers of the endosperm, whereas larger cells occupied the central region (Fig. 5A), in agreement with previous observations that the sizes of both the nuclei and the cells increase from the aleurone layer to the central endosperm in different maize lines (Tschermak-Woess and Enzenberg-Kunz, 1965; Kowles and Phillips, 1988; Larkins et al., 2001). The layers of endosperm cells lining the embryo pocket contained larger cells at higher endopolyploidy levels than the outer endosperm layers away from the embryo in both genotypes (Fig. 5, A and B).

The central endosperm cells can only expand rapidly during crown development if cell growth is coordinated with enlargement of the endosperm surface, sustained by anticlinal divisions of the peripheral cells (Kiesselbach, 1949). The surface of the endosperm, without the embryo pocket and the basal region, was about 40 mm^2 in the wild-type kernel but only 15 mm^2 in the *miniature*, as estimated from the 3-D model. Because the size of cells in the outer most layer was similar in both genotypes, the estimated number of these outer cells was about three times lower in the *miniature* than in the wild-type endosperm. Thus, it seems likely that impaired mitosis in the peripheral layers of the *miniature* endosperm imposes physical constraints upon expansion of the central cells. Indeed, regarding the same pattern of endoreduplication process in the *miniature* endosperm and in the wild type (Fig. 3), *miniature* cells at respective endopolyploidy levels were smaller than expected (Fig. 4B).

The lower levels of metabolically released, osmotically active sugars (hexoses) and precursors for cell wall biosynthesis available to the *miniature* endosperm due to the INCW2 deficiency may lead to a reduced cell expansion in the peripheral region. This may, in turn, cause a reduced mitotic activity in the outer cell layers through cell size control mechanisms, in agreement with the hypothesis of "expansion leads mitosis" (Jacobs, 1997). INCW2 deficiency may also result in a premature high ratio of Suc to hexose in the endosperm, which may favor cell differentiation and starch accumulation over cell division, as has been shown for fava bean (Weber et al., 1997). Although the mechanisms involved in regulation of cell cycle and differentiation in relation to sugar levels are presently largely unknown, the presented results support the hypothesis that the role of cell wall invertase in control of seed development in maize is similar to its regulatory role described in fava bean (Weber et al., 1997).

ACKNOWLEDGMENTS

In memoriam of Profs. Elisabeth Tschermak-Woess (1917–2001) and Oliver E. Nelson (1920–2001).

Received December 18, 2001; returned for revision January 23, 2002; accepted February 7, 2002.

LITERATURE CITED

Cheng WH, Chourey PS (1999) Theor Appl Genet **98:** 485–495

Cheng WH, Taliercio EW, Chourey PS (1996). Plant Cell **8:** 971–983

Greilhuber J, Ebert I (1994) Genome **37:** 646–655

Jacobs T (1997) Plant Cell **9:** 1021–1029

Jones RJ, Roessler J, Quattar S (1985) Crop Sci **25:** 830–834

Kiesselbach TA (1949) Research Bulletin 161. Agricultural Experiment Station, University of Nebraska, Lincoln

Kondorosi E, Roudier F, Gendreau E (2000) Curr Opin Plant Biol **3:** 488–492

Kowles RV, McMullen MD, Yerk G, Phillips RL, Kraemer S, Srienc F (1992) Genome **35:** 68–77
Kowles RV, Phillips RL (1985) Proc Natl Acad Sci USA **82:** 7010–7014
Kowles RV, Phillips RL (1988) Int Rev Cytol **112:** 97–136
Larkins BA, Dilkes BP, Dante RA, Coelho CM, Woo Y, Liu Y (2001) J Exp Bot **52:** 183–192
Lowe J, Nelson OE Jr (1946) Genetics **31:** 525–533
Matérn B (1960) Medd Statens Skogsforskningsinst **49:** 1–144
Miller ME, Chourey PS (1992) Plant Cell **4:** 297–305
Sagan C (1997) Billions and Billions. Headline Book Publishing, London
Schweizer L, Yerk-Davis GL, Phillips RL, Srienc F, Jones RJ (1995) Proc Natl Acad Sci USA **92:** 7070–7074
Settler TL, Flannigan BA (2001) J Exp Bot **52:** 1401–1408
Tsai CY, Salamini F, Nelson OE (1970) Plant Physiol **46:** 299–306
Tschermak-Woess E, Enzenberg-Kunz U (1965). Planta **64:** 149–169
Vilhar B, Dermastia M (2002) Acta Bot Croat **61:** 11–25
Vilhar B, Greilhuber J, Dolenc Koce J, Temsch EM, Dermastia M (2001) Ann Bot **87:** 719–728
Weber H, Borisjuk L, Wobus U (1997) Trends Plant Sci **2:** 169–174